Taylor & Francis
Taylor & Francis Group

RESEARCH ARTICLE

# Effects of dacomitinib on the pharmacokinetics of poziotinib *in vivo* and *in vitro*

Weiping Ji[a]*, Jiquan Shen[a]*, Bo Wang[a], Feifei Chen[b], Deru Meng[b], Shuanghu Wang[b,c], Dapeng Dai[d], Yunfang Zhou[b], Changxiong Wang[e] and Quan Zhou[b]

[a]Department of Orthopaedics, The Sixth Affiliated Hospital of Wenzhou Medical University, The People's Hospital of Lishui, Lishui, China; [b]The Laboratory of Clinical Pharmacy, The Sixth Affiliated Hospital of Wenzhou Medical University, The People's Hospital of Lishui, Lishui, China; [c]School of Pharmaceutical Science, Guangdong Provincial Key Laboratory of New Drug Screening, Southern Medical University, Guangzhou, China; [d]The Key Laboratory of Geriatrics, Beijing Institute of Geriatrics, Beijing Hospital, National Center of Gerontology, National Health Commission, Institute of Geriatric Medicine, Chinese Academy of Medical Sciences, Beijing, China; [e]Department of Gastroenterology, The Sixth Affiliated Hospital of Wenzhou Medical University, The People's Hospital of Lishui, Lishui, China

## ABSTRACT

**Context:** Dacomitinib and poziotinib, irreversible ErbB family blockers, are often used for treatment of non-small cell lung cancer (NSCLC) in the clinic.

**Objective:** This study investigates the effect of dacomitinib on the pharmacokinetics of poziotinib in rats.

**Materials and methods:** Twelve Sprague–Dawley rats were randomly divided into two groups: the test group (20 mg/kg dacomitinib for 14 consecutive days) and the control group (equal amounts of vehicle). Each group was given an oral dose of 10 mg/kg poziotinib 30 min after administration of dacomitinib or vehicle at the end of the 14 day administration. The concentration of poziotinib in plasma was quantified by UPLC-MS/MS. Both *in vitro* effects of dacomitinib on poziotinib and the mechanism of the observed inhibition were studied in rat liver microsomes and human liver microsomes.

**Results:** When orally administered, dacomitinib increased the AUC, $T_{max}$ and decreased CL of poziotinib ($p < 0.05$). The $IC_{50}$ values of M1 in RLM, HLM and CYP3A4 were 11.36, 30.49 and 19.57 μM, respectively. The $IC_{50}$ values of M2 in RLM, HLM and CYP2D6 were 43.69, 0.34 and 0.11 μM, respectively, and dacomitinib inhibited poziotinib by a mixed way in CYP3A4 and CYP2D6. The results of the *in vivo* experiments were consistent with those of the *in vitro* experiments.

**Conclusions:** This research demonstrates that a drug–drug interaction between poziotinib and dacomitinib possibly exists when readministered with poziotinib; thus, clinicians should pay attention to the resulting changes in pharmacokinetic parameters and accordingly, adjust the dose of poziotinib in clinical settings.

## Introduction

The tyrosine kinase inhibitor (TKI) family is a family of oral epidermal growth factor receptor drugs that inhibit the activity of tyrosine kinase. This family can be roughly divided into three types, reversible EGFR-TKIs (such as erlotinib and gefitinib), irreversible ErbB family blockers (poziotinib and dacomitinib) and mutant-selective EGFR-TKIs (AZD9291, CO-1686 and HM6171) (Leong et al. 2017; Koga et al. 2018; Belgin et al. 2019; Kim Y et al. 2019). Dacomitinib is representative of highly selective reversible EGFR-TKIs, including HER1, HER2 and HER4 (Qiu et al. 2019). It has previously been reported that dacomitinib has a significant therapeutic effect on patients with advanced non-small cell lung cancer (NSCLC) with EGFR-activating mutations, gastric cancer and neck squamous cell carcinoma (Abdul Razak et al. 2013; Oh et al. 2016; Kim DW et al. 2017). In addition, Yu et al. (2019) observed that dacomitinib reduces pulmonary artery pressure and relieves right ventricular hypertrophy. Several previous experiments have indicated that

dacomitinib is mainly mediated by CYP2D6 and, to a lesser extent, by CYP3A4 and CYP2C9 (Peters et al. 2014; Giri et al. 2015; Chen et al. 2018). Additionally, dacomitinib is a substrate for CYP2D6 and an inhibitor of CYP2D6. The metabolism of dacomitinib varies across different ethnic groups and foods (Ramalingam et al. 2014). Research by Bello et al. (2012) indicated that the combined use of dacomitinib and the drug metabolized by CYP2D6 can have a significant impact on the pharmacokinetics of subjects with an extensive metabolism for CYP2D6. An experiment Ruiz-Garcia et al. (2014) discovered that, when coadministered with paroxetine, which is a potent CYP3A4 inhibitor, dacomitinib exposure increased by 37% in healthy volunteers. When taken every day, the modest effect of dacomitinib is unlikely to be clinically significant.

Poziotinib (HM781-36B) is a novel oral irreversible panhuman EGF receptor (HER) TKI, and it has a stronger inhibitory effect on EGFR than that of other EGFR tyrosine kinase inhibitors, including EGFR-acquired resistance mutation (T790M), HER2 and HER4 (Nam et al. 2011). Poziotinib is clinically used

CONTACT Quan Zhou ✉ zhouquan1991@lsu.edu.cn; Yunfang Zhou ✉ zyf2808@lsu.edu.cn 🖃 The Laboratory of Clinical Pharmacy, The Sixth Affiliated Hospital of Wenzhou Medical University, The People's Hospital of Lishui, Lishui 323000, China; Changxiong Wang ✉ wangchenbo2006@163.com 🖃 Department of Gastroenterology, The Sixth Affiliated Hospital of Wenzhou Medical University, The People's Hospital of Lishui, Lishui 323000, China
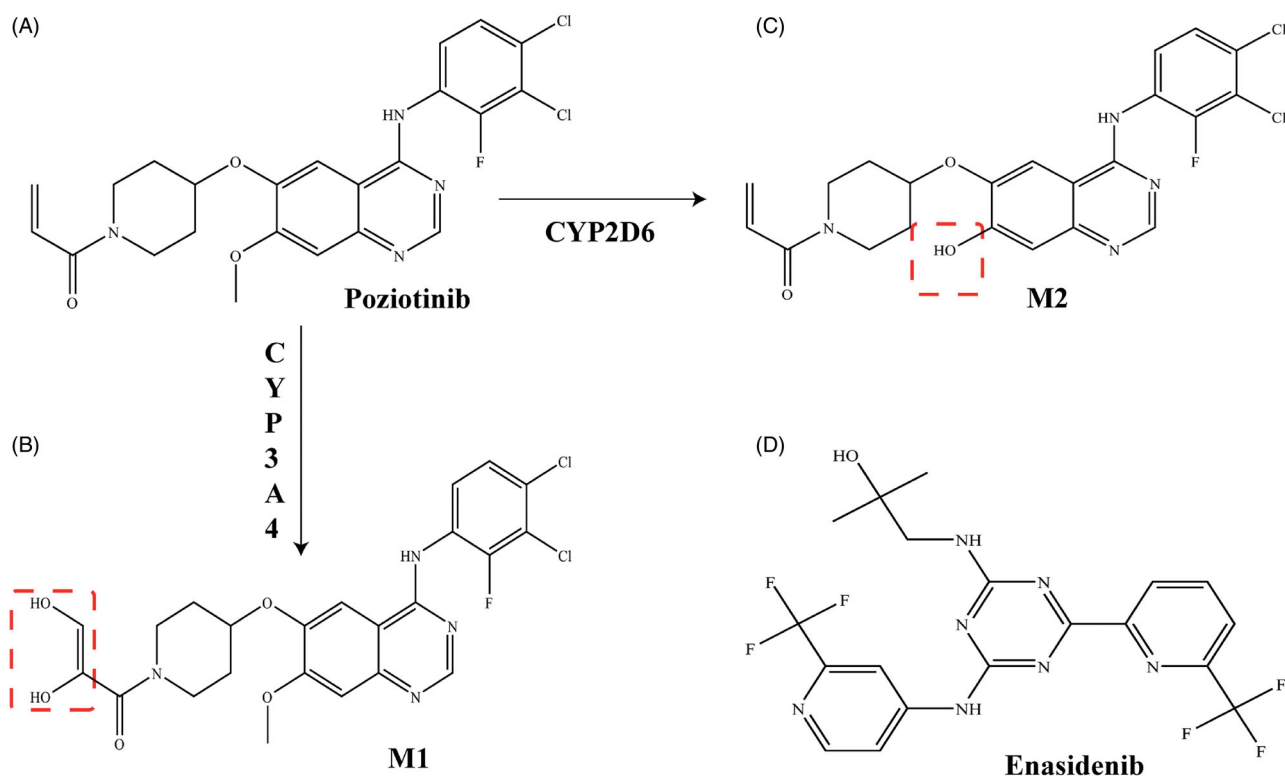*These authors contributed equally to this work.

**Figure 1.** Chemical structures of poziotinib (A), M1 (B), M2 (C) and enasidenib (D).

for treating a variety of advanced solid tumours, including non-small cell lung cancer (NSCLC) with EGFR mutations (T790M), breast cancer, and gastric cancer (Cha et al. 2012; Park et al. 2018; Kim JY et al. 2019). Kim et al. (2013) reported that HM781-36B is mainly metabolised by CYP3A4 (mainly M1) and partially metabolized by CYP2D6 (mainly M2), which they determined via *in vitro* and *in vivo* experiments (Figure 1). In other words, using the representative HPLC chromatograms of HM781-36B incubation products in HLM, human recombinant CYP3A4, and CYP2D6 at 254 nm, they concluded that the main metabolites of HM781-36B were M1, M2, M8 and M10 and the minor metabolites of HM781-36B were M3, M4, M5, M6, M7 and M9. Noh et al. (2015) demonstrated that, aside from weight, HM781-36 pharmacokinetics were not affected by other patient factors (including sex, height medical history, tumour types, etc.). Although, in their study, HM781-36 was administered regardless of food intake, no study has been performed on the effect of drugs on HM781-36. Considering the pharmacokinetic characteristics of dacomitinib and poziotinib, we hypothesize that when dacomitinib is administered for several days prior to taking poziotinib, the metabolism of poziotinib *in vivo* may be altered. The effect may be increased adverse reactions, such as diarrhoea, stomatitis, cheilitis, conjunctivitis and anorexia (Kimura et al. 2017; Kim et al. 2018).

The purpose of this experiment was to investigate the effects of dacomitinib on the pharmacokinetics of poziotinib *in vivo* and *in vitro*. The pharmacokinetic parameters of poziotinib in rats with or without dacomitinib pre-treatment were analyzed using a sensitive and reliable UPLC-MS/MS system *in vivo*. The effect of dacomitinib on poziotinib in rat liver microsomes was determined. Additionally, the peak areas of the two major metabolite products (M1 and M2) of poziotinib were measured *in vitro* (Noh et al. 2015; Cheong et al. 2017).

## Materials and methods

### Chemicals and reagents

Dacomitinib (purity > 98%), poziotinib (purity > 98%) and enasidenib (IS purity > 98%) were purchased from the Beijing Sunflower and Technology Development Co. Ltd. (Beijing, China). Acetonitrile and methanol were purchased from Fisher Scientific Co. (Fair Lawn, NJ, USA). Formic acid was purchased from Sigma-Aldrich (St. Louis, MO, USA). Ultrapure water was obtained from a Milli-Q water purification system (Millipore, Billerica, MA, USA). Carboxy methylcellulose sodium salt (CMC-Na) was from Sinopharm Chemical Reagent Co. Ltd (Shanghai China). Food was purchased from Shenyang Maohua Biotechnology Co. Ltd (Shenyang China). The reduced form of nicotinamide adenine dinucleotide phosphate was purchased from Roche Co. Ltd (Shanghai China). HLM were purchased from Corning Co. Ltd (Woburn, MA, USA). RLM were obtained from our laboratory. All other chemicals were of analytical grade or better.

### Instruments and conditions

The concentrations of poziotinib were determined on a UPLC-MS/MS system, which possessed an ACQUITY I Class UPLC and a XEVO TQD triple quadrupole mass spectrometer (Waters Corp., Milford, MA, USA). The UPLC system consists of a Binary Solvent Manager (BSM) and a Sample Manager with Flow-Through Needle (SM-FTN). Chromatographic analysis of poziotinib was performed on a CORTECS C18 column (2.1 × 50 mm, 1.6 μm) maintained at 40 °C. The mobile phase consisted of 0.1% formic acid and acetonitrile, and the elution process had a linear gradient: It started with acetonitrile

increasing from 10 to 30% (0–1 min); rapidly increasing from 30 to 95% (1–2 min), which was maintained at 95% (2–2.5 min); and then decreasing to 10% (2.5–2.6 min). The flow rate was 0.4 mL/min, and the total run time was 3 min. The precursor ion and product ion, which were determined by the positive MRM mode, were $m/z$ 492.06→354.55 and $m/z$ 474.57→456.64 for poziotinib and IS, respectively. The optimal MS parameters were defined as follows: the cone voltages were both set at 30 V for poziotinib and IS; the collision energies were set at 20 and 28 eV for poziotinib and IS, respectively.

### Animals and treatment

Sprague–Dawley rats were obtained from the experimental animal centre of Wenzhou Medical University (Wenzhou China). The animals were housed in a breeding room at 25 °C with $60 \pm 5\%$ humidity and a 12 h dark/light cycle. Water and diet were provided ad libitum. The Sprague–Dawley rats were acclimated to the above conditions for two weeks before initiating the animal experiment. All of the experimental procedures were approved by the Animal Experimental Ethical Inspection of Laboratory Animal Centre, Wenzhou Medical University and followed the guidelines for the care and use of laboratory animals (ID Number: wydw2019-650).

### Pharmacokinetic experiment

Twelve Sprague–Dawley rats weighing $240 \pm 10$ g were selected and divided into two groups ($n = 6$). The groups were as follows: the control group and the test group. First, dacomitinib was dissolved in a CMC-Na solution. Then, 20 mg/kg/day dacomitinib was orally administered once daily to the test group for two weeks, while equal amounts of vehicle (normal CMC-Na solution) were orally administered to the control group. Thirty minutes later, each group of rats was given an oral dose of 10 mg/kg poziotinib (dissolved in CMC-Na solution) at the end of the 14 day administration. A 50 μL aliquot of blood was collected from the rat tail vein at 0.167, 0.5, 1, 2, 3, 4, 6, 8, 12, 24 and 36 h after poziotinib administration. To the collected blood, 20 μL of IS and 100 μL of acetonitrile were added in a 1.5 mL microcentrifuge tube. The mixture was vortexed for 30 s and then centrifuged at 13,000 rpm for 5 min. Subsequently, the supernatants were removed and placed in a sample bottle. Supernatant (5 μL) was immediately analysed using a sensitive and reliable LC-MS/MS method.

### In vitro experiments

The procedure for preparing RLM was based on the methods of Marques et al. (2014). The 200 μL incubation system contained 2 μM poziotinib; 0.44 mg/mL RLM, 5 pmol recombinant human CYP3A4 or 5 pmol recombinant human CYP2D6; 1 mM NADPH; and 100 mM potassium phosphate buffer (PH 7.4) and

dacomitinib. To determine the $IC_{50}$ of dacomitinib for inhibiting poziotinib metabolism, the concentration of dacomitinib was set as 0.01, 0.1, 1, 5, 10,50 and 100 μM, while that of poziotinib was 100 μM for 0.44 mg/mL RLM, 0.28 mg/mL HLM, 5 pmol recombinant human CYP3A4 or 5 pmol recombinant human CYP2D6, which was close to its $K_m$ value. To determine the mechanisms underlying the inhibitory effect of dacomitinib on poziotinib based on the $IC_{50}$ and $K_m$ value, 0, 5, 10, 20, 50 and 100 μM of dacomitinib, and 1, 2.5, 5, 10 and 20 μM of poziotinib were selected in the RLM system; 0, 7.5, 15, 30 and 60 μM of dacomitinib, and 1, 2.5, 5 and 10 μM of poziotinib were selected in the HLM system.

The incubation was performed at 37 °C for 50 min, followed by cooling to −80 °C to terminate reaction at the same time, after which 400 μL of acetonitrile and 20 μL of IS (50 ng/mL) were added to the mixture. After vortex mixing for 30 s and centrifugation at 13,000 rpm for 5 min, the supernatant was obtained for LC-MS/MS analysis.

### Statistical analysis

The pharmacokinetic parameters, including the maximal plasma concentration ($C_{max}$), the maximum plasma time ($T_{max}$), the apparent volume of distribution ($Vz/F$), the area under the plasma concentration-time curve (AUC), the elimination half-life ($t_{1/2}$), the plasma clearance (CL) and the mean residence time (MRT), were analyzed using DAS (Drug and Statistics) software (Version 3.2.8, The People's Hospital of Lishui, China). The $IC_{50}$ and Lineweaver–Burk plot were obtained using GraphPad Prism (Version 7; GraphPad Software Inc., San Diego, CA, USA).

All of the pharmacokinetic parameters are expressed as the mean ± SD. Statistical analyses of the main pharmacokinetic parameters were performed using the independent sample Student's $t$-test using SPSS (version 16.0; SPSS Inc., Chicago, IL, USA). Values of $p < 0.05$ were considered to be statistically significant.

## Results

### Method validation and LC-MS/MS

The validation procedures for selectivity, linearity, accuracy, precision, recovery and stability referred to the European Medicines Agency Guidelines and US-FDA Bioanalytical Method Validation Guidance (Ma et al. 2015; Wang SH et al. 2015, 2016; Wang XQ et al. 2015; Kaza et al. 2019). The inter- and intraday precision, accuracy, recovery and matrix of poziotinib in rat plasma are shown in Table 1. The chromatograms of a blank plasma sample, a blank plasma sample added to poziotinib (LLOQ) and IS, and a plasma sample after the oral administration of poziotinib are shown in Figure 2. The concentrations of the calibration curves ranged from 1 to 1000 ng/mL for poziotinib, with both correlation coefficients over 0.9907. The LLOQ was set at 1 ng/mL for poziotinib with acceptable accuracy and precision.

Table 1. Inter- and intraday precision, accuracy, recovery and matrix of poziotinib in rat plasma ($n = 6$, mean ± SD).

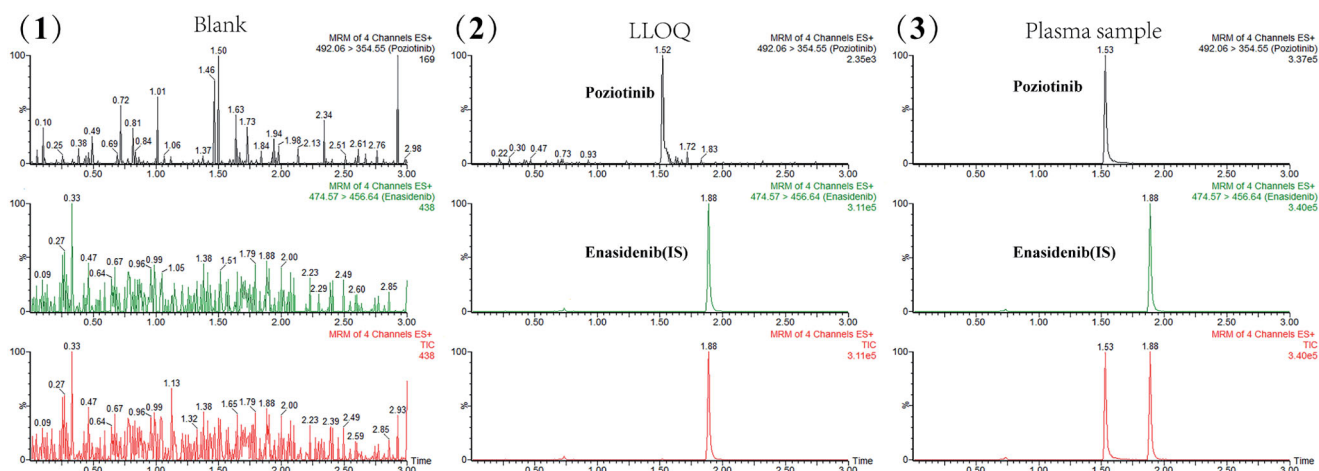| Analyte | Nominal concentration (ng/mL) | Intraday | | Interday | | Recovery (%) | Matrix (%) |
| | | Precision RSD (%) | Accuracy RE (%) | Precision RSD (%) | Accuracy RE (%) | | |
| --- | --- | --- | --- | --- | --- | --- | --- |
| Poziotinib | 1 | 14.00 | 106.42 | 9.85 | 102.54 | | |
| | 2 | 7.47 | 108.44 | 8.67 | 109.38 | 81.80 | 85.36 |
| | 80 | 7.77 | 106.84 | 5.27 | 105.72 | 96.42 | 87.71 |
| | 800 | 6.49 | 107.46 | 9.52 | 102.62 | 93.58 | 91.94 |

**Figure 2.** MRM chromatograms of poziotinib and IS. (1) Blank plasma sample, (2) blank plasma sample with poziotinib (LLOQ) and IS, and (3) plasma sample 2 h after dosing poziotinib with oral administration.
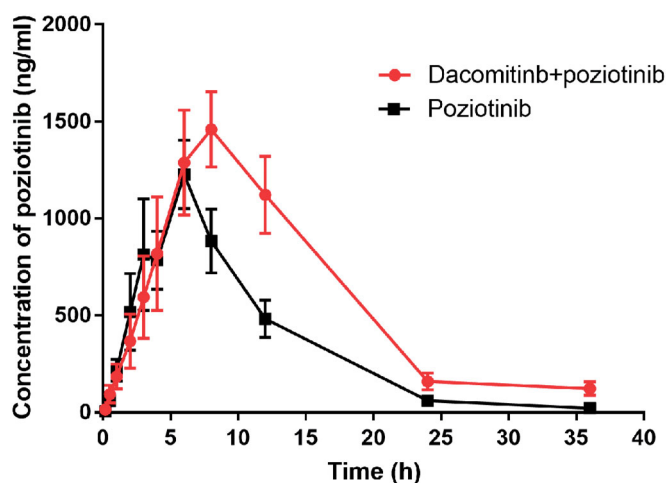


**Figure 3.** Mean plasma concentration–time curves of poziotinib in the test and control groups.

### Effects of dacomitinib on the pharmacokinetics of poziotinib *in vivo*

The mean plasma concentration-time curves of poziotinib in the test (preadministered dacomitinib) and control (equal amounts of vehicle) groups are shown in Figure 3. The corresponding pharmacokinetic parameters are summarised in Table 2. Comparing the test group with the control group, the $AUC_{(0-t)}$ of poziotinib was increased by 1.6-fold, and the difference was significant ($p < 0.01$). When preadministered with dacomitinib (10 mg/kg) for two weeks, the $T_{max}$ and $t_{1/2}$ values of poziotinib were significantly increased by 1.3- and 1.6-fold, respectively. Compared with the control group, the values of $MRT_{(0-t)}$, $MRT_{(0-\infty)}$ and $AUC_{(0-\infty)}$ of poziotinib were increased while the value of $CLz/F$ was decreased. The $C_{max}$ and $Vz/F$ values of poziotinib were not greatly changed by pre-treatment with dacomitinib ($p > 0.05$).

### Effects of dacomitinib on the pharmacokinetics of poziotinib *in vitro*

Michaelis–Menten kinetics of poziotinib in RLM and HLM were shown in Figure 4. The inhibitory effect of dacomitinib on poziotinib in RLM, HLM, CYP2D6 and CYP3A4 were

**Table 2.** Main pharmacokinetic parameters of poziotinib in the two groups ($n = 6$, mean ± SD).

| Pharmacokinetics parameters | Control group | Test group | *p*-Values |
|---|---|---|---|
| AUC(0–t) (μg/L h) | 12506.44 ± 1981.29 | 20920.85 ± 2579.95** | 0.000 |
| AUC(0–∞) (μg/L h) | 12597.80 ± 1994.45 | 22212.70 ± 2217.34** | 0.000 |
| MRT(0–t) (h) | 9.01 ± 0.400 | 11.40 ± 0.83** | 0.000 |
| MRT(0–∞) (h) | 9.26 ± 0.51 | 13.56 ± 2.22** | 0.001 |
| t1/2z (h) | 4.53 ± 0.85 | 7.45 ± 1.64** | 0.003 |
| Tmax (h) | 6.00 ± 0.00 | 7.67 ± 0.82** | 0.001 |
| Vz/F (L/kg) | 5.31 ± 1.36 | 4.92 ± 1.37 | 0.639 |
| CLz/F (L/h/kg) | 0.81 ± 0.12 | 0.45 ± 0.05** | 0.000 |
| Cmax (μg/L) | 1226.67 ± 176.84 | 1461.01 ± 192.05 | 0.053 |

*$p < 0.05$; **$p < 0.01$ indicate significant differences from the control.
AUC, area under the plasma concentration–time curve; CL, plasma clearance; $C_{max}$, maximum plasma concentration; MRT, mean residence time; SD, standard deviation; $t_{1/2}$, half-life; $T_{max}$, maximum plasma time; *Vz/F*: apparent volume of distribution.

investigated according to the peak area ratio of metabolites of poziotinib (M1 and M2). The $IC_{50}$ values of poziotinib are shown in Figure 5. The mechanism of inhibition by dacomitinib in RLM and HLM are illustrated by the Lineweaver–Burk plot shown in Figure 6. The $IC_{50}$ values and inhibitory effects of dacomitinib on poziotinib metabolism are shown in Table 3. The $IC_{50}$ values of M1 in RLM, HLM and CYP3A4 were 11.36, 30.49 and 19.57 μM, respectively. The $IC_{50}$ values of M2 in RLM, HLM and CYP2D6 were 43.69, 0.34 and 0.11 μM, respectively. The $K_i$, and $\alpha K_i$ values of M1 in RLM are 8.18, and 38.81 μM, respectively. The $K_i$, and $\alpha K_i$ values of M2 in RLM are 47.48, and 38.07 μM, respectively. The $K_i$, and $\alpha K_i$ values of M1 in HLM are 83.74 and 93.73 μM, respectively. The $K_i$, and $\alpha K_i$ values of M2 in HLM are 0.17, and 0.66 μM, respectively. These results indicated that dacomitinib was a mixed inhibitor of poziotinib in RLM and HLM. Moreover, the inhibitory effect was different for all enzymes, especially CYP2D6.

### Discussion

The purpose of this research was to demonstrate alterations in the pharmacokinetics of poziotinib after the administration of dacomitinib in rats. The results indicated that this method could be used for the analysis of poziotinib in rats and in rat liver microsome samples, which could meet the European Medicines
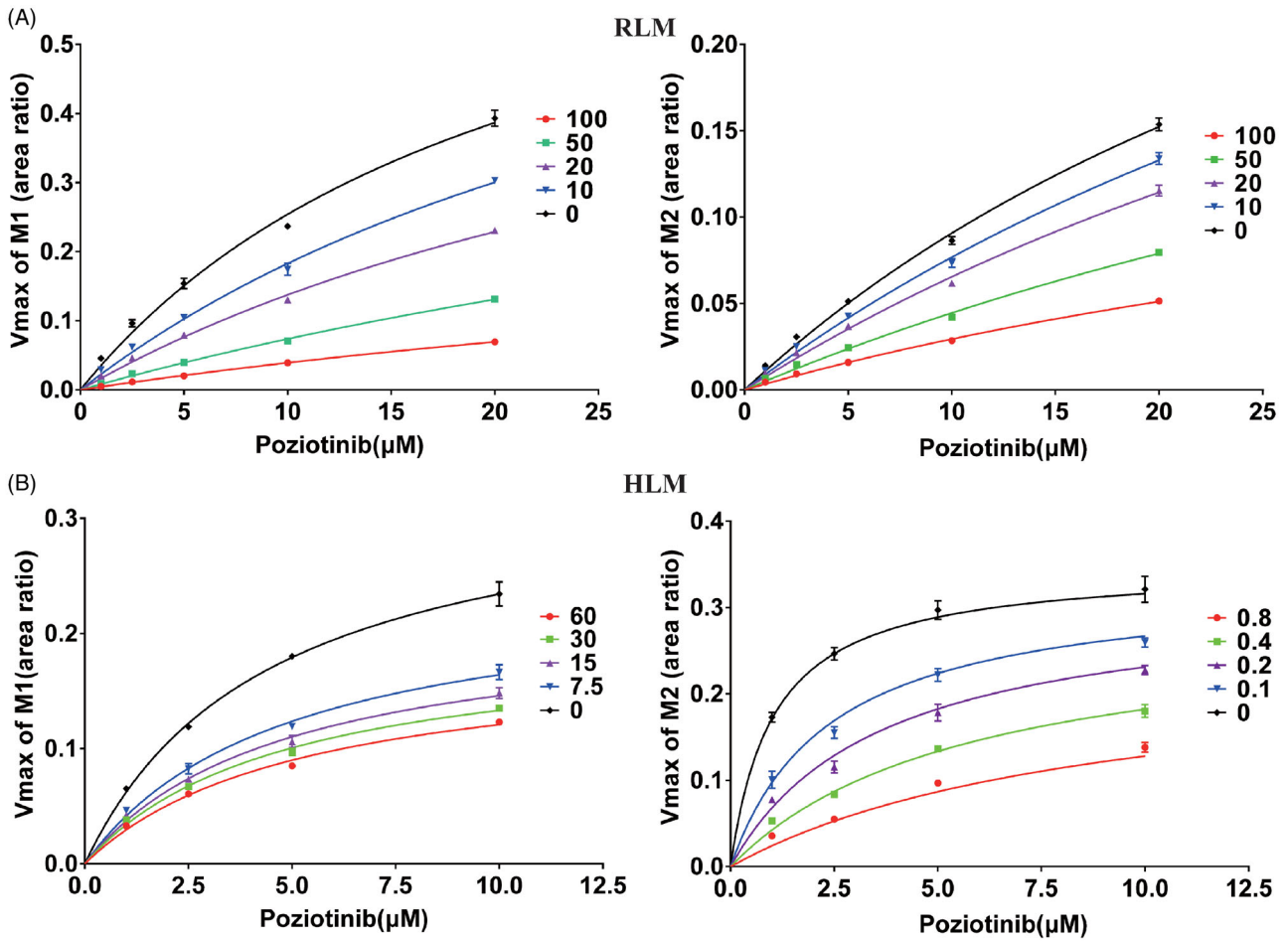
**Figure 4.** Michaelis–Menten kinetics of poziotinib in RLM (A) and HLM (B).
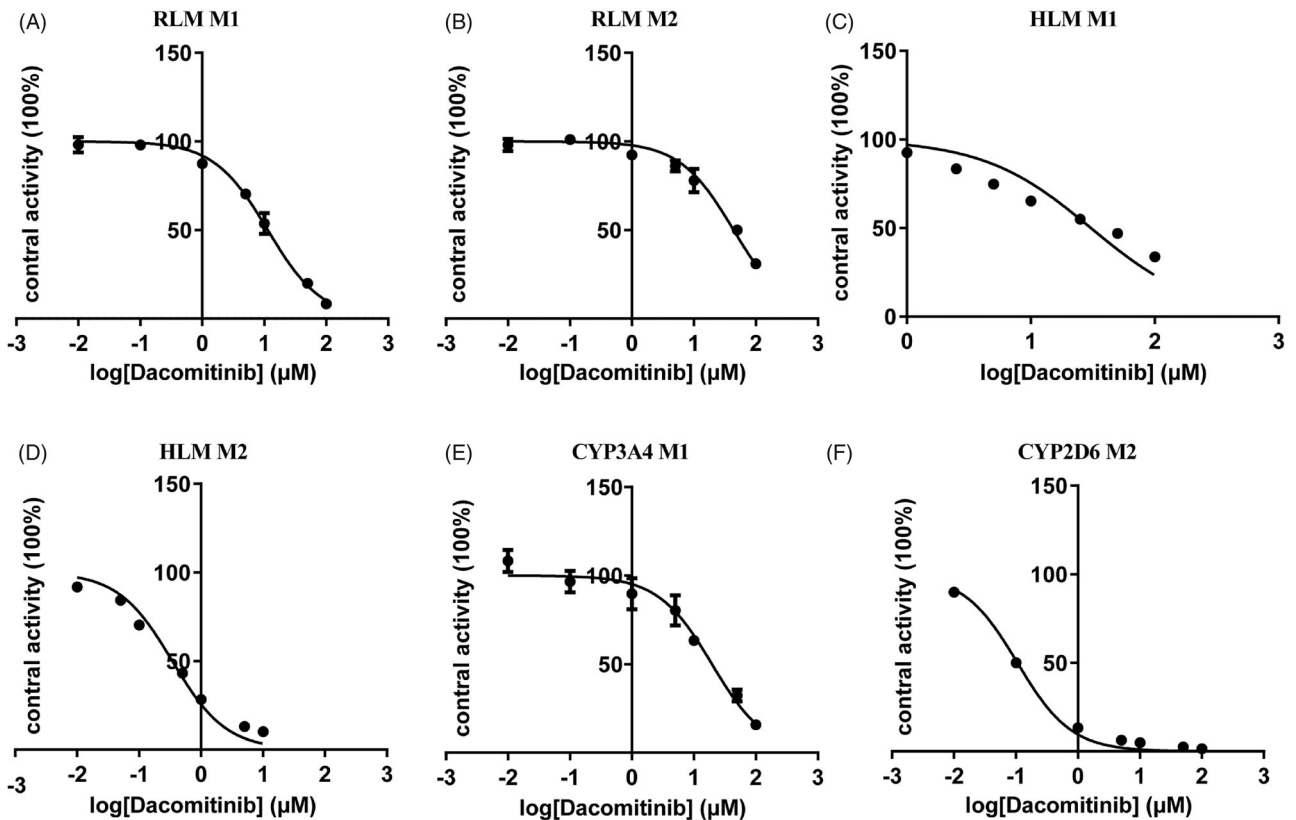


**Figure 5.** Poziotinib with various concentrations to determine the $IC_{50}$ for the activity of RLM (A, B), HLM (C, D), CYP3A4 (E) and CYP2D6 (F).
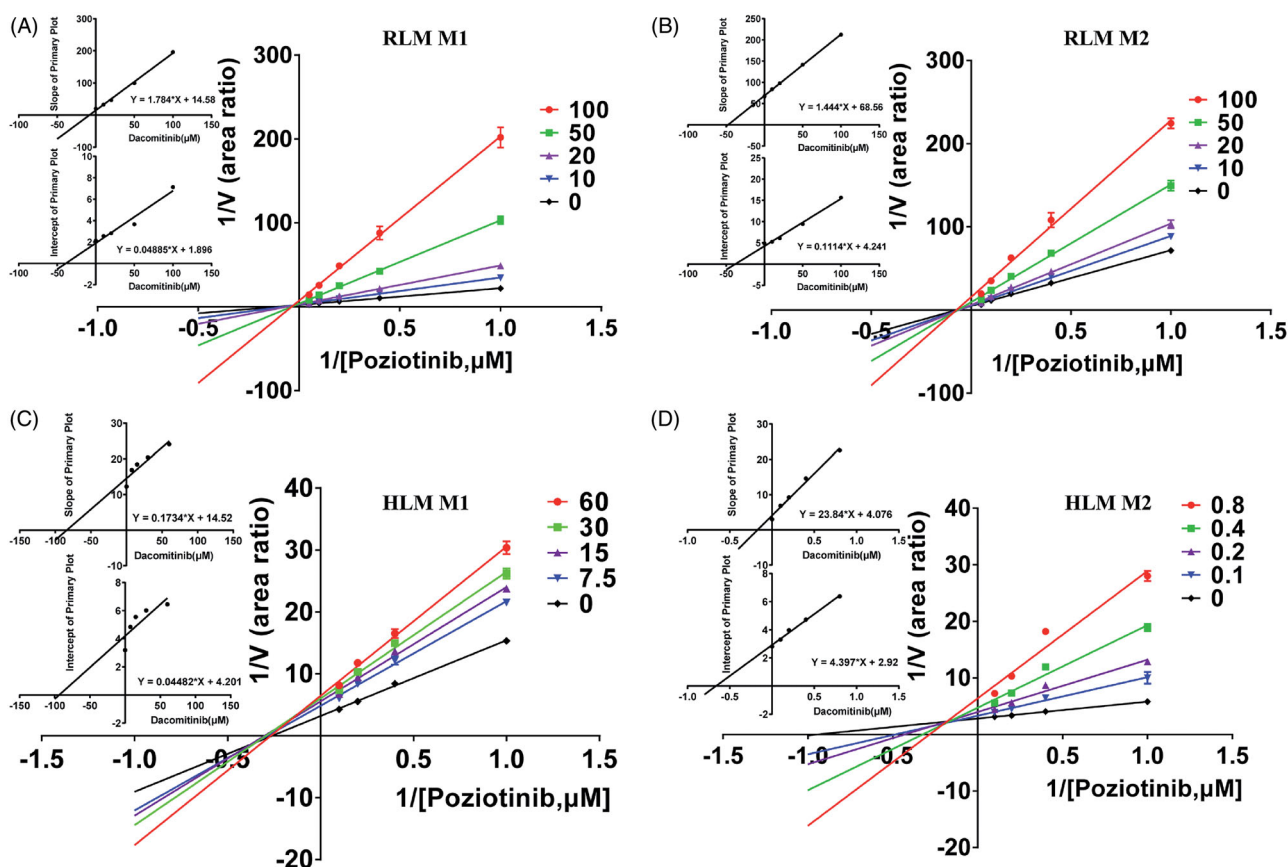
**Figure 6.** Lineweaver–Burk plots and the secondary plot for $K_i$ of the inhibition of poziotinib metabolism by dacomitinib in RLM (A, B) and HLM (C, D).

**Table 3.** The $IC_{50}$ values and inhibitory effects of dacomitinib on poziotinib metabolism in RLM, HLM, CYP3A4 and CYP2D6.

| | | $IC_{50}$ values (µM) | Inhibition type | $K_i$ (µM) | $\alpha K_i$ (µM) | $\alpha$ |
|---|---|---|---|---|---|---|
| RLM | M1 | 21.77 | Mixed | 8.18 | 38.81 | 4.74 |
| | M2 | 90.14 | Mixed | 47.48 | 38.07 | 0.81 |
| HLM | M1 | 30.49 | Mixed | 83.74 | 93.73 | 1.12 |
| | M2 | 0.34 | Mixed | 0.17 | 0.66 | 3.88 |
| CYP3A4 | M1 | 19.57 | | | | |
| CYP2D6 | M2 | 0.11 | | | | |

Agency Guidelines and US-FDA Bioanalytical Method Validation Guidance. After oral administration, poziotinib was slowly absorbed by plasma and reached a maximum concentration at 6 h in rats. Poziotinib was quickly eliminated from plasma with an elimination $t_{1/2}$ of $4.53 \pm 0.85$ h. Currently, pharmacokinetic studies of poziotinib in rats are lacking. Although Kim et al. (2013) studied the plasma concentration-time curves of poziotinib in dogs after an oral dose of 0.3 mg/kg poziotinib, the $T_{max}$ and $t_{1/2}$ values of poziotinib were 0.40–1.00 h and 3.40–5.40 h, respectively. In conclusion, the pharmacokinetic parameters of poziotinib in dogs and rats were significantly different.

The interaction between drugs is generally determined according to pharmacokinetic properties, and it occurs in the phase of absorption, distribution, metabolism or excretion (Kim TH et al. 2017; Qin et al. 2017; Darbalaei et al. 2018). Drug–drug interactions, which can produce irrelevant, synergistic, additive, and antagonistic results, are increasingly recognized as important clinical events. When rats were pre-treated with dacomitinib, the extent of absorption of poziotinib was significantly increased, and its performance was determined by the $AUC_{(0-\infty)}$, which ranged from $12597.80 \pm 1994.45$ µg/L/h to $22212.70 \pm 2217.34$ µg/L/h. In parallel, the $T_{max}$ value of poziotinib was delayed by nearly 3 h after pre-treatment with dacomitinib. Compared to control rats, the pharmacokinetic parameters in metabolism ($t_{1/2}$) were significantly increased in rats that were pre-treated with dacomitinib. These data indicate that the pharmacokinetics of poziotinib are significantly affected by dacomitinib in rats. We performed *in vitro* experiments to further evaluate the effect of dacomitinib on the pharmacokinetics of poziotinib metabolites. Cheong et al. (2017) predicted drug interactions between rivaroxaban and antiarrhythmic drugs *in vivo* and *in vitro* by applying Static Modelling. In this study, we measured the peak area ratios of two major metabolites of poziotinib using the same method and finally obtained the $IC_{50}$ values of M1 and M2 by conversion. According to the $IC_{50}$ values of M1 and M2, it can indicate that dacomitinib mainly inhibited the metabolism of poziotinib by inhibiting the metabolism of the CYP2D6 metabolic enzyme in HLM, while it by inhibiting CYP3A4 in RLM. One reason explanation of the difference in $IC_{50}$ values between HLM and RLM is the species difference between humans and rats. Our results also show that dacomitinib not only fully inhibit CYP2D6, but also can inhibit CYP3A4. Furthermore, the Lineweaver–Burk plot suggested that the inhibition was of a mixed type, which included competitive and non-competitive inhibition ($K_i \neq \alpha K_i$). The results showed that dacomitinib has a clear inhibitory effect on poziotinib metabolism *in vitro*, which agrees with the *in vivo* results.

From the previously mentioned results, it is known that CYP3A4 and CYP2D6 participates in the metabolism of poziotinib. There might be the potential for clinically significant interactions with modulators of the CYP450 enzyme to alter plasma concentrations when coadministered, potentially leading to

enhanced adverse effects (Danton et al. 2013; Samer et al. 2013). Poziotinib is a novel antitumor drug, and changes in its plasma concentration can cause serious adverse reactions (Romero 2018). In a phase I/II study of poziotinib combined with pacli-taxel and trastuzumab, Kim TY et al. (2019) evaluated the safety and tolerability of poziotinib and defined the maximum tolerated dose (MTDs) of poziotinib as 8 mg/day. In a phase I study of poziotinib in patients with advanced solid tumours, Kim et al. (2018) proposed that the MTDs of poziotinib in the continuous or intermittent dosing schedule were 18 or 24 mg/day, respect-ively. The main adverse reactions of poziotinib were diarrhoea, rash, stomatitis and pruritus in their experiments. No obvious adverse effects were observed in our study, the different findings could be due to the differences in metabolic enzymes and the physiological conditions between rats and human (Martignoni et al. 2006). The pharmacokinetics of poziotinib was significantly change by dacomitinib in rats, it provided a reference for the clinical when they are co-administered.

## Conclusions

The data from this study clearly illustrate the pharmacokinetics of poziotinib and the role that dacomitinib plays in the pharma-cokinetic change of poziotinib. When orally administered, daco-mitinib could increase the AUC, prolong the $t_{1/2}$, and decrease the CL of poziotinib. Our results also indicate that the inhibition of poziotinib metabolism by dacomitinib may be of mixed type. Consequently, since dacomitinib has an inhibitory effect on CYP2D6, an inhibitory effect on poziotinib was observed. The results of this experiment were based on rat models. Given the differences in metabolic enzymes and the physiological condi-tions between species, further human studies are needed.

## Author contributions

Quan Zhou, Weiping Ji, Changxiong Wang and Bo Wang conceived and designed the experiments; Bo Wang, Feifei Chen, Jiquan Shen, Quan Zhou and Deru Meng performed the experiments; Quan Zhou, Jiquan Shen and Feifei Chen analysed the data; Shuanghu Wang, and Yunfang Zhou contributed reagents/materials/analysis tools; and Bo Wang, Jiquan Shen and Shuanghu Wang wrote the paper. All the authors read and approved the final manuscript.

## Disclosure statement

None of the authors have any conflicts of interest related to this paper.

## Funding

## References

Abdul Razak AR, Soulieres D, Laurie SA, Hotte SJ, Singh S, Winquist E, Chia S, Le Tourneau C, Nguyen-Tan PF, Chen EX, et al. 2013. A phase II trial of dacomitinib, an oral pan-human EGF receptor (HER) inhibitor, as first-line treatment in recurrent and/or metastatic squamous-cell carcin-oma of the head and neck. Ann Oncol. 24(3):761–769.

Belgin S, Altı ntop MD, Radwan MO, Özdemir A, Otsuka M, Fujita M, Ciftci 2019. Design, synthesis and biological evaluation of a new series of thiazolyl-pyrazolines as dual EGFR and HER2 inhibitors. Eur J Med Chem. 182:111648–111681.

Bello CL, LaBadie RR, Ni G, Boutros T, McCormick C, Ndongo MN. 2012. The effect of dacomitinib (PF-00299804) on CYP2D6 activity in healthy volunteers who are extensive or intermediate metabolizers. Cancer Chemother Pharmacol. 69(4):991–997.

Cha MY, Lee KO, Kim M, Song JY, Lee KH, Park J, Chae YJ, Kim YH, Suh KH, Lee GS, et al. 2012. Antitumor activity of HM781-36B, a highly effective pan-HER inhibitor in erlotinib-resistant NSCLC and other EGFR-dependent cancer models. Int J Cancer. 130(10):2445–2454.

Chen X, Jiang J, Giri N, Hu P. 2018. Phase 1 study to investigate the phar-macokinetic properties of dacomitinib in healthy adult Chinese subjects genotyped for CYP2D6. Xenobiotica. 48(5):459–466.

Cheong EJ, Goh JJ, Hong Y, Venkatesan G, Liu Y, Chiu GN, Kojodjojo P, Chan EC. 2017. Application of static modeling -in the prediction of in vivo drug-drug interactions between rivaroxaban and antiarrhythmic agents based on in vitro inhibition studies. Drug Metab Dispos. 45(3): 260–268.

Danton AC, Montastruc F, Sommet A, Durrieu G, Bagheri H, Bondon-Guitton E, Lapeyre-Mestre M, Montastruc JL. 2013. Importance of cyto-chrome P450 (CYP450) in adverse drug reactions due to drug-drug inter-actions: a PharmacoVigilance study in France. Eur J Clin Pharmacol. 69(4):885–888.

Darbalaei S, Zhang X, Wang N, Qin Y, Han X, Rang Y, Zhai X, Lu Y. 2018. Effects of aprepitant on the pharmacokinetics of imatinib and its main metabolite in rats. Pharmazie. 73(6):329–334.

Giri N, Masters JC, Plotka A, Liang Y, Boutros T, Pardo P, O'Connell J, Bello C. 2015. Investigation of the impact of hepatic impairment on the pharmacokinetics of dacomitinib. Invest New Drugs. 33(4):931–941.

Kaza M, Karaźniewicz-Łada M, Kosicka K, Siemiątkowska A, Rudzki PJ. 2019. Bioanalytical method validation: new FDA guidance vs. EMA guide-line. Better or worse? J Pharm Biomed Anal. 165:381–385.

Kim DW, Garon EB, Jatoi A, Keefe DM, Lacouture ME, Sonis S, Gernhardt D, Wang T, Giri N, Doherty JP, et al. 2017. Impact of a planned dose interruption of dacomitinib in the treatment of advanced non-small-cell lung cancer (ARCHER 1042). Lung Cancer. 106:76–82.

Kim E, Kim H, Suh K, Kwon S, Lee G, Park NH, Hong J. 2013. Metabolite identification of a new tyrosine kinase inhibitor, HM781-36B, and a phar-macokinetic study by liquid chromatography/tandem mass spectrometry. Rapid Commun Mass Spectrom. 27(11):1183–1195.

Kim JY, Lee E, Park K, Jung HH, Park WY, Lee KH, Sohn J, Lee KS, Jung KH, Kim JHm, et al. 2019. Molecular alterations and poziotinib efficacy, a pan-HER inhibitor, in human epidermal growth factor receptor 2 (HER2)-positive breast cancers: combined exploratory biomarker analysis from a phase II clinical trial of poziotinib for refractory HER2-positive breast cancer patients. Int J Cancer. 145(6):1669–1678.

Kim TH, Shin S, Kim S, Bulitta JB, Weon KY, Joo SH, Ma E, Yoo SD, Park GY, Kwon DR, et al. 2017. Alterations in pharmacokinetics of gemcitabine and erlotinib by concurrent administration of Hyangsayukgunja-Tang, a gastroprotective herbal medicine. Molecules. 22(9):1515–1528.

Kim TY, Han HS, Lee KW, Zang DY, Rha SY, Park YI, Kim JS, Lee KH, Park SH, Song EK, et al. 2019. A phase I/II study of poziotinib combined with paclitaxel and trastuzumab in patients with HER2-positive advanced gastric cancer. Gastric Cancer. 22(6):1206–1214.

Kim TM, Keun-Wook L, Do-Youn O, Jong-Seok L, Seock-Ah I, Dong-Wan K, Sae-Won H, Yu Jung K, Tae-You K, Jee Hyun K, et al. 2018. Phase 1 Studies of poziotinib, an irreversible pan-HER tyrosine kinase inhibitor in patients with advanced solid tumors. Cancer Res Treat. 50(3):835–842.

Kim Y, Kim Y, Lee S, Yang H, Kim S. 2019. Personalized prediction of acquired resistance to EGFR-targeted inhibitors using a pathway-based machine learning approach. Cancers. 11(1):45–58.

Kimura K, Takayanagi R, Fukushima T, Yamada Y. 2017. Theoretical method for evaluation of therapeutic effects and adverse effects of epidermal growth factor receptor tyrosine kinase inhibitors in clinical treatment. Med Oncol. 34(10):178.

Koga T, Kobayashi Y, Tomizawa K, Suda K, Kosaka T, Sesumi Y, Fujino T, Nishino M, Ohara S, Chiba M, et al. 2018. Activity of a novel HER2 inhibitor, poziotinib, for HER2 exon 20 mutations in lung cancer and mechanism of acquired resistance: an in vitro study. Lung Cancer. 126: 72–79.

Leong S, Moss RA, Bowles DW, Ware JA, Zhou J, Spoerke JM, Lackner MR, Shankar G, Schutzman JL, van der Noll R, et al. 2017. A Phase I dose-escalation study of the safety and pharmacokinetics of pictilisib in

combination with erlotinib in patients with advanced solid tumors. Oncologist. 22(12):1491–1499.

Ma JS, Wang SH, Huang XL, Geng PW, Wen CC, Zhou YF, Yu LS, Wang XQ. 2015. Validated UPLC-MS/MS method for determination of hordenine in rat plasma and its application to pharmacokinetic study. J Pharm Biomed Anal. 111:131–137.

Marques LM, da Silva EA, Jr, Gouvea DR, Vessecchi R, Pupo MT, Lopes NP, Kato MJ, de Oliveira AR. 2014. *In vitro* metabolism of the alkaloid piplartine by rat liver microsomes. J Pharm Biomed Anal. 95:113–120.

Martignoni M, Groothuis GM, de Kanter R. 2006. Species differences between mouse, rat, dog, monkey and human CYP-mediated drug metabolism, inhibition and induction. Expert Opin Drug Metab Toxicol. 2(6): 875–894.

Nam HJ, Kim HP, Yoon YK, Hur HS, Song SH, Kim MS, Lee GS, Han SW, Im SA, Kim TY, et al. 2011. Antitumor activity of HM781-36B, an irreversible Pan-HER inhibitor, alone or in combination with cytotoxic chemotherapeutic agents in gastric cancer. Cancer Lett. 302(2):155–165.

Noh YH, Lim HS, Jung JA, Song TH, Bae KS. 2015. Population pharmacokinetics of HM781-36 (poziotinib), pan-human EGF receptor (HER) inhibitor, and its two metabolites in patients with advanced solid malignancies. Cancer Chemother Pharmacol. 75(1):97–109.

Oh DY, Lee KW, Cho JY, Kang WK, Im SA, Kim JW, Bang YJ. 2016. Phase II trial of dacomitinib in patients with HER2-positive gastric cancer. Gastric Cancer. 19(4):1095–1103.

Park YH, Lee KH, Sohn JH, Lee KS, Jung KH, Kim JH, Lee KH, Ahn JS, Kim TY, Kim GM, et al. 2018. A phase II trial of the pan-HER inhibitor poziotinib, in patients with HER2-positive metastatic breast cancer who had received at least two prior HER2-directed regimens: results of the NOV120101-203 trial. Int J Cancer. 143(12):3240–3247.

Peters S, Zimmermann S, Adjei AA. 2014. Oral epidermal growth factor receptor tyrosine kinase inhibitors for the treatment of non-small cell lung cancer: comparative pharmacokinetics and drug-drug interactions. Cancer Treat Rev. 40(8):917–926.

Qin X, Lu J, Wang P, Xu P, Liu M, Wang X. 2017. Cytochrome P450 3A selectively affects the pharmacokinetic interaction between erlotinib and docetaxel in rats. Biochem Pharmacol. 143:129–139.

Qiu X, Lin Q, Ning Z, Qian X, Li P, Ye L, Xie S. 2019. Quantitative bioanalytical assay for the human epidermal growth factor receptor (HER) inhibitor dacomitinib in rat plasma by UPLC-MS/MS. J Pharm Biomed Anal. 166:66–70.

Ramalingam SS, Jänne PA, Mok T, O'Byrne K, Boyer MJ, Von Pawel J, Pluzanski A, Shtivelband M, Docampo LI, Bennouna J, et al. 2014. Dacomitinib versus erlotinib in patients with advanced-stage, previously treated non-small-cell lung cancer (ARCHER 1009): a randomised, double-blind, phase 3 trial. The Lancet Oncology. 15(12):1369–1378.

Romero D. 2018. Poziotinib for uncommon ERBB mutations. Nat Rev Clin Oncol. 15(7):404–404.

Ruiz-Garcia A, Giri N, LaBadie RR, Ni G, Boutros T, Richie N, Kocinsky HS, Checchio TM, Bello CL. 2014. A phase I open-label study to investigate the potential drug-drug interaction between single-dose dacomitinib and steady-state paroxetine in healthy volunteers. J Clin Pharmacol. 54(5): 555–562.

Samer CF, Lorenzini KI, Rollason V, Daali Y, Desmeules JA. 2013. Applications of CYP450 testing in the clinical setting. Mol Diagn Ther. 17(3):165–184.

Wang SH, Wu HY, Geng PW, Lin YY, Liu ZZ, Zhang LJ, Ma JS, Zhou YF, Wang XQ, Wen CC. 2016. Pharmacokinetic study of dendrobine in rat plasma by ultra-performance liquid chromatography tandem mass spectrometry. Biomed Chromatogr. 30(7):1145–1149.

Wang SH, Wu HY, Huang XL, Geng PW, Wen CC, Ma JS, Zhou YF, Wang XQ. 2015. Determination of N-methylcytisine in rat plasma by UPLC-MS/ MS and its application to pharmacokinetic study. J Chromatogr B Analyt Technol Biomed Life Sci. 990:118–124.

Wang XQ, Wang SH, Lin FY, Zhang QW, Chen HL, Wang XC, Wen CC, Ma JS, Hu LF. 2015. Pharmacokinetics and tissue distribution model of cabozantinib in rat determined by UPLC-MS/MS. J Chromatogr B Analyt Technol Biomed Life Sci. 983–984:125–131.

Yu X, Zhao X, Zhang J, Li Y, Sheng P, Ma C, Zhang L, Hao X, Zheng X, Xing Y, et al. 2019. Dacomitinib, a new pan-EGFR inhibitor, is effective in attenuating pulmonary vascular remodeling and pulmonary hypertension. Eur J Pharmacol. 850:97–108.